

SCIENTIFIC REPORTS



OPEN

Excellent magnetocaloric properties in RE_2Cu_2Cd ($RE = Dy$ and Tm) compounds and its composite materials

Received: 13 July 2016
Accepted: 08 September 2016
Published: 26 September 2016

Yikun Zhang¹, Yang Yang¹, Xiao Xu¹, Shuhua Geng¹, Long Hou¹, Xi Li¹, Zhongming Ren¹ & Gerhard Wilde²

The magnetic properties and magnetocaloric effect (MCE) of ternary intermetallic RE_2Cu_2Cd ($RE = Dy$ and Tm) compounds and its composite materials have been investigated in detail. Both compounds undergo a paramagnetic to ferromagnetic transition at its own Curie temperatures of $T_C \sim 48.5$ and 15 K for Dy_2Cu_2Cd and Tm_2Cu_2Cd , respectively, giving rise to the large reversible MCE. An additionally magnetic transition can be observed around 16 K for Dy_2Cu_2Cd compound. The maximum values of magnetic entropy change ($-\Delta S_M^{max}$) are estimated to be 17.0 and 20.8 J/kg K for Dy_2Cu_2Cd and Tm_2Cu_2Cd , for a magnetic field change of 0 – 70 kOe, respectively. A table-like MCE in a wide temperature range of 10 – 70 K and enhanced refrigerant capacity (RC) are achieved in the Dy_2Cu_2Cd - Tm_2Cu_2Cd composite materials. For a magnetic field change of 0 – 50 kOe, the maximum improvements of RC reach 32% and 153% , in comparison with that of individual compound Dy_2Cu_2Cd and Tm_2Cu_2Cd . The excellent MCE properties suggest the RE_2Cu_2Cd ($RE = Dy$ and Tm) and its composite materials could be expected to have effective applications for low temperature magnetic refrigeration.

Magnetic refrigeration technology based on the magnetocaloric effect (MCE) shows superior application potential over conventional gas compression/expansion refrigeration technology because of its environmental friendliness, higher energy efficiency as well as compactness^{1–5}. The MCE is an intrinsic thermal response for the application or removal of a magnetic field to a magnetic material, which can be characterized by the coupled variations of two quantities: the adiabatic temperature change (ΔT_{ad}) or/and isothermal magnetic entropy change (ΔS_M). To satisfy practical application, extensive efforts have been carried out to pick out the magnetic materials with large/giant MCE as magnetic refrigerants^{1–10}.

Recently, the rare-earth (RE) based alloys and oxides, which exhibit the large reversible MCEs and refrigeration capacity with small or zero hysteresis have been of great interest^{11–17}. Increasing efforts have been devoted for study of the ternary intermetallic compounds of the $RE_2T_2X_{2:2:1}$ ($T =$ transition metals, and $X =$ III group p-metals). Among of the $2:2:1$ system, the RE_2Cu_2X ($X = Mg, Cd, Sn$ or In) crystallized with the tetragonal Mo_2B_2Fe -type structure¹⁸, have attracted some attentions because of their unique physical and magnetic properties. The basic crystal chemical data of the different RE_2T_2X series have been reviewed^{19,20}. Very recently, Zhang *et al.* and Li *et al.* have reported the large reversible MCEs in RE_2Cu_2In ($RE = Dy, Er$, and Tm) and Ho_2T_2In ($T = Cu$ and Au) compounds, respectively^{21–23}. However, the systems with the p-metals as cadmium are much less known, what besides other reasons could be explained also by the difficulty in materials synthesis due to the high vapour pressure (low boiling point) of cadmium.

To further understand the physical properties of RE_2T_2X system, in this paper, the magnetic properties and MCE in RE_2Cu_2Cd ($RE = Dy$ and Tm) compounds and its composite materials have been investigated systematically. Not only a large reversible MCE was observed in Dy_2Cu_2Cd and Tm_2Cu_2Cd compounds, but also an enhanced refrigerant capacity was found in its composite materials.

¹State Key Laboratory of Advanced Special Steels & Shanghai Key Laboratory of Advanced Ferrometallurgy & School of Materials Science and Engineering, Shanghai University, 200072, China. ²Institute of Materials Physics, University of Münster, Wilhelm-Klemm-Straße 10, D-48149 Münster, Germany. Correspondence and requests for materials should be addressed to Y.Z. (email: ykzhang10@hotmail.com) or X.L. (email: lx_net@sina.com)

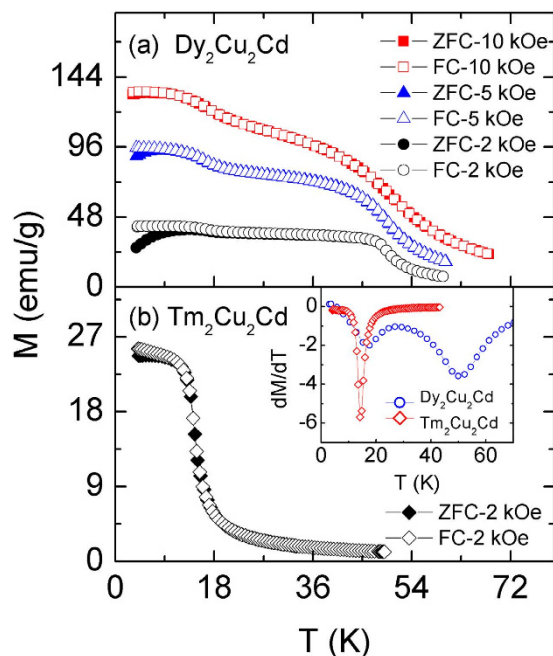


Figure 1. Temperature dependence zero-field cooling (ZFC) and field cooling (FC) magnetization (M) under different magnetic fields for $\text{Dy}_2\text{Cu}_2\text{Cd}$ (a) and the magnetic field of 2 kOe for $\text{Tm}_2\text{Cu}_2\text{Cd}$ (b) compounds, respectively. Inset of (b) shows the temperature dependence dM_{FC}/dT for $\text{Dy}_2\text{Cu}_2\text{Cd}$ and $\text{Tm}_2\text{Cu}_2\text{Cd}$ compounds under the magnetic field of 2 kOe.

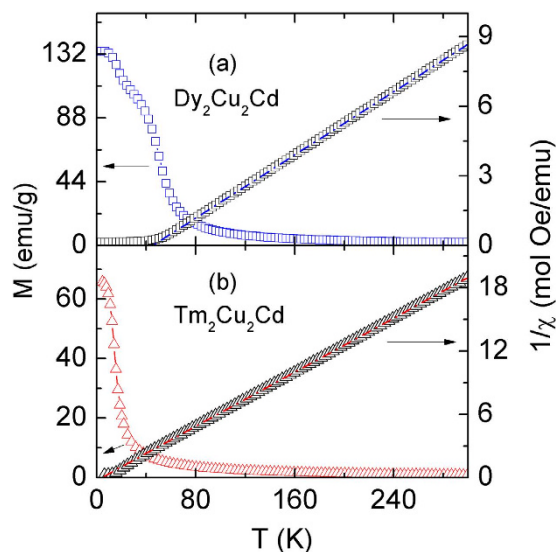


Figure 2. Temperature dependence of magnetization (M , left scale) and the reciprocal susceptibility ($1/\chi$, right scale) for $\text{Dy}_2\text{Cu}_2\text{Cd}$ (a) and $\text{Tm}_2\text{Cu}_2\text{Cd}$ (b) compounds under the magnetic field of $H = 10$ kOe, respectively.

Results and Discussion

Figure 1(a,b) show the temperature dependence of the zero field cooled (ZFC) and field cooled (FC) magnetization M under different magnetic fields for $\text{Dy}_2\text{Cu}_2\text{Cd}$ and a magnetic field of 2 kOe for $\text{Tm}_2\text{Cu}_2\text{Cd}$, respectively. Both compounds display a typical paramagnetic to ferromagnetic (PM-FM) transition, and the Curie temperatures T_C , corresponding to the peak of $dM_{\text{FC}}/dT - T$ curve [inset of Fig. 1(b)], are determined to be 48.5 K and 15 K for $\text{Dy}_2\text{Cu}_2\text{Cd}$ and $\text{Tm}_2\text{Cu}_2\text{Cd}$, respectively. Another magnetic transition can be observed for $\text{Dy}_2\text{Cu}_2\text{Cd}$ around $T_S \sim 16$ K under low magnetic fields and it shifts to much lower temperatures with increasing magnetic field. Such behaviours may arise from a spin glass transition or spin reorientation phenomenon^{24,25}, a systematically detail study of the lower temperature magnetic transition will be performed later. The transition temperatures are in good agreement with previously reported values in the literatures²⁰. Figure 2(a,b) show the temperature dependence of the magnetization M (left side) and the reciprocal susceptibility $1/\chi$ (right side) for $\text{Dy}_2\text{Cu}_2\text{Cd}$ and

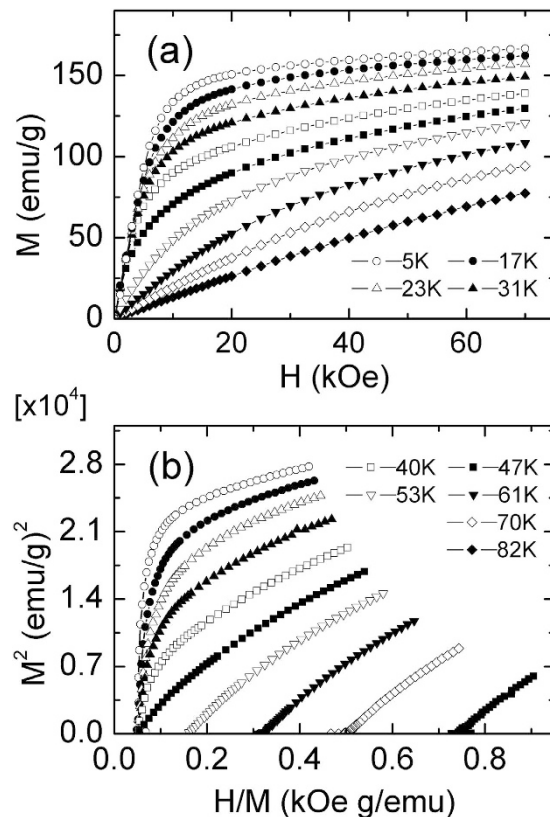


Figure 3. (a) Magnetic field dependence of the magnetization (increasing field only) for $\text{Dy}_2\text{Cu}_2\text{Cd}$ at some selected temperatures. (b) The plots of H/M versus M^2 for $\text{Dy}_2\text{Cu}_2\text{Cd}$ at some selected temperatures.

$\text{Dy}_2\text{Cu}_2\text{Cd}$ compounds under a magnetic field of 10 kOe, respectively. The $1/\chi$ in paramagnetic regime from 80 to 298 K obeys the Curie-Weiss law for both compounds. The fitted lines are a guide to the eyes for $\text{Dy}_2\text{Cu}_2\text{Cd}$ and $\text{Tm}_2\text{Cu}_2\text{Cd}$ compounds as shown in the insets of Fig. 2(a,b), respectively. The fit to the Curie-Weiss formula yields positive paramagnetic Curie temperatures (θ_p), $\theta_p = 45.3$ K for $\text{Dy}_2\text{Cu}_2\text{Cd}$ and $\theta_p = 14.1$ K for $\text{Tm}_2\text{Cu}_2\text{Cd}$, respectively, suggesting dominant ferromagnetic interactions. The effective magnetic moments (μ_{eff}) are $10.84 \mu_B$ and $7.72 \mu_B$ for $\text{Dy}_2\text{Cu}_2\text{Cd}$ and $\text{Tm}_2\text{Cu}_2\text{Cd}$, respectively. Such moments are close to those of the free ion values of Dy and Tm taking the theoretical RE^{3+} moment of $10.86 \mu_B$ and $7.56 \mu_B$, respectively.

The magnetic isothermal $M(H)$ curves of $\text{Dy}_2\text{Cu}_2\text{Cd}$ and $\text{Tm}_2\text{Cu}_2\text{Cd}$ compounds with increasing field around their transition temperatures with increasing magnetic field up to 70 kOe have been measured and some of them are shown in Figs 3(a) and 4(a), respectively. The magnetization below T_C increases rapidly in the low magnetic field range for both compounds, and it tends to saturate for $\text{Dy}_2\text{Cu}_2\text{Cd}$ compound with increasing magnetic field, whereas it is not saturated at 70 kOe for $\text{Tm}_2\text{Cu}_2\text{Cd}$ compound. To further understand the magnetic transitions, Arrott plots (H/M vs. M^2) of $\text{Dy}_2\text{Cu}_2\text{Cd}$ and $\text{Tm}_2\text{Cu}_2\text{Cd}$ compounds are shown in Figs 3(b) and 4(b), respectively. According to Banerjee criterion²⁶, the signal (positive and negative) of the slope in Arrott plots has been used to determine the nature of the magnetic phase transition. The negative slopes or inflection points in the Arrott plots often are corresponding to a first order phase transition, whereas the positive slopes are associated to a second order phase transition. By this criterion, neither the inflection points nor negative slopes can be observed in the Arrott plots for $\text{Dy}_2\text{Cu}_2\text{Cd}$ and $\text{Tm}_2\text{Cu}_2\text{Cd}$ compounds, indicating a characteristic of the second order (FM-PM) magnetic phase transition.

Figure 5(a,b) show the temperature dependence of magnetic entropy change $-\Delta S_M$ for $\text{Dy}_2\text{Cu}_2\text{Cd}$ and $\text{Tm}_2\text{Cu}_2\text{Cd}$ compounds which is derived from the temperature and field dependence of the magnetization $M(H, T)$ by using the Maxwell's thermodynamic relation²⁷, $\Delta S_M(T, \Delta H) = \int_0^{\Delta H} (\partial M(H, T) / \partial T)_H dH$, respectively. It can be found that the maximum value of $-\Delta S_M$ increases monotonically with increasing magnetic field change for both compounds [see insets of Fig. 5(a,b)]. Two successive $-\Delta S_M$ peaks (one at around T_C , another at around T_S) can be clearly seen even the low magnetic field change for $\text{Dy}_2\text{Cu}_2\text{Cd}$ compound, thus obviously enlarging the temperature range of MCE. Only a pronounced peak in the $-\Delta S_M(T)$ curves is observed around T_C for $\text{Tm}_2\text{Cu}_2\text{Cd}$ compound. For the magnetic field changes of 0–20, 0–50, and 0–70 kOe, the maximum values of the magnetic entropy change ($-\Delta S_M^{\text{max}}$) are evaluated to be 7.2, 13.8, and 17.0 J/kg K around T_C , and 3.3, 6.6, and 8.3 J/kg K around T_S for $\text{Dy}_2\text{Cu}_2\text{Cd}$ compound; and to be 9.2, 17.3 and 20.8 J/kg K for $\text{Tm}_2\text{Cu}_2\text{Cd}$ compound, respectively.

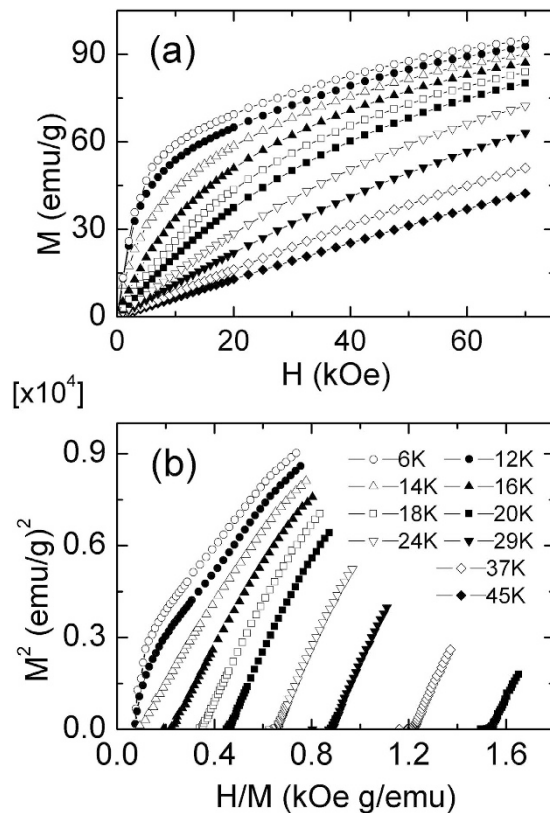


Figure 4. (a) Magnetic field dependence of the magnetization (increasing field only) for $\text{Tm}_2\text{Cu}_2\text{Cd}$ at some selected temperatures. (b) The plots of H/M versus M^2 for $\text{Tm}_2\text{Cu}_2\text{Cd}$ at some selected temperatures.

In addition, the $\Delta S_M(T)$ curves for the materials with the second order phase transition can be also described using a universal curve^{28,29}, which is constructed by normalizing with their respective maximum value ΔS_M^{max} (i. e. $\Delta S' = \Delta S_M(T)/\Delta S_M^{\text{max}}$) and rescaling the temperature θ , defined as

$$\theta = \begin{cases} -(T - T_C)/(T_{r1} - T_C), & T \leq T_C \\ (T - T_C)/(T_{r2} - T_C), & T > T_C \end{cases} \quad (1)$$

where the T_{r1} and T_{r2} are the temperatures of the two reference points of each curve that correspond to $0.6\Delta S_M^{\text{max}}$. The transformed $\Delta S'(\theta)$ curves for $\text{Tm}_2\text{Cu}_2\text{Cd}$ and $\text{Dy}_2\text{Cu}_2\text{Cd}$ compounds are displayed in Figs 6 and 7, respectively. We can note that all the rescaled ΔS_M curves for $\text{Tm}_2\text{Cu}_2\text{Cd}$ are overlapped with each other in the present temperature range, as shown in Fig. 6, proving the occurrence of the second order magnetic phase transition in $\text{Tm}_2\text{Cu}_2\text{Cd}$ compound. In parallel, the curves for $\text{Dy}_2\text{Cu}_2\text{Cd}$ compound are also overlapped with each other around and above T_C (see Fig. 7). Whereas an obvious deviation below T_C for $\theta < -2$ (around T_S) can be found which is properly due to the spin reorientation phenomenon or spin glass transition. Therefore, the $\Delta S_M(T)$ around T_S (5–30 K) are rescaled and the results are shown in the inset of Fig. 7. Similarly, the curves around T_S are well overlapped with each other. Furthermore, the rescaled $\Delta S'(\theta)$ curves around T_C and T_S for $\text{Dy}_2\text{Cu}_2\text{Cd}$ compound under various magnetic field changes are summarized together (as given in the Fig. 8). One can find that all the rescaled ΔS_M curves can collapse onto one universal curve, which is consistent with the previous investigations that the materials with successive magnetic phase transitions^{22,24,30,31}. The analysis of the universal behaviour further confirms that the $\text{Dy}_2\text{Cu}_2\text{Cd}$ compound with the second order phase transition.

Another important quality factor of refrigerant materials is the refrigerant capacity [RC, defined as numerically integrating the area under the $-\Delta S_M - T$ curve at full width of half maximum (δ_{FWHM}) of the $-\Delta S_M$ peak as the integrating limits]. For the magnetic field changes of 0–20, 0–50, and 0–70 kOe, the values of RC are evaluated to be 87, 316, and 495 J/kg for $\text{Dy}_2\text{Cu}_2\text{Cd}$ compound; and to be 60, 165, and 248 J/kg for $\text{Tm}_2\text{Cu}_2\text{Cd}$ compound, respectively. It is well known that magnetic refrigeration systems based on an ideal Ericsson cycle requires a magnetocaloric material with a constant ΔS_M over an operating refrigeration temperature range^{32,33}. Besides the materials with successive magnetic transitions or with a very magnetic field sensitive magnetic phase transitions^{22,24,30,31,34}, composite materials have been considered to be the most promising method to accomplish the requirement of Ericsson cycle since it can lead to almost constant ΔS_M with enlarged temperature span^{35–38}. An enhanced RC have been successfully realized in $\text{Eu}_8\text{Ga}_{16}\text{Ge}_{30}\text{-EuO}$ ³⁶, amorphous FeZrB(Cu) ³⁷, and ErNiBC-GdNiBC ³⁸ composite materials. We can note that the $\text{Dy}_2\text{Cu}_2\text{Cd}$ and $\text{Tm}_2\text{Cu}_2\text{Cd}$ compounds possess the same crystal structure with similar lattice parameters and similar magnitudes of the magnetic entropy change ($-\Delta S_M$). Therefore, these composite materials could be expected to fulfil the required Ericsson cycle conditions.

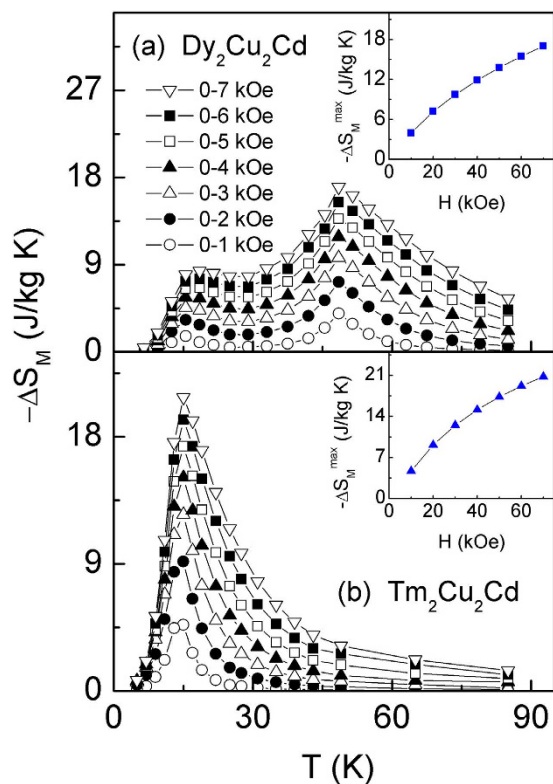


Figure 5. The magnetic entropy change $-\Delta S_M$ as a function of temperature for various magnetic field changes ΔH up to 0–70 kOe for $\text{Dy}_2\text{Cu}_2\text{Cd}$ (a) and $\text{Tm}_2\text{Cu}_2\text{Cd}$ (b) compounds, respectively. Insets of (a,b) show the maximum values of magnetic entropy change ($-\Delta S_M^{\text{max}}$) as a function of the magnetic field changes for $\text{Dy}_2\text{Cu}_2\text{Cd}$ and $\text{Tm}_2\text{Cu}_2\text{Cd}$ compounds, respectively.

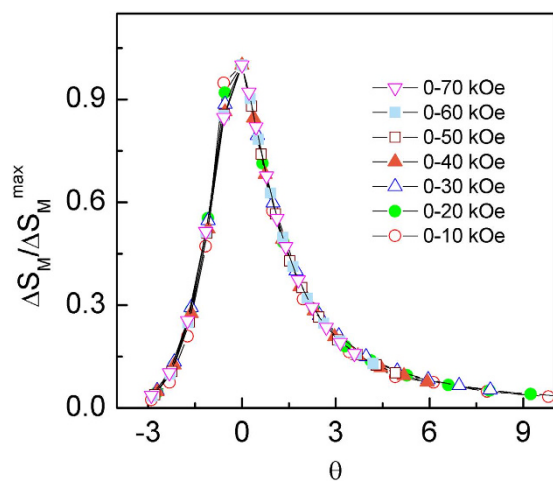


Figure 6. Normalized magnetic entropy change $\Delta S'_M (= \Delta S_M / \Delta S_M^{\text{max}})$ as a function of the rescaled temperature θ in the present temperature range for $\text{Tm}_2\text{Cu}_2\text{Cd}$ compound.

The total magnetic entropy change of $x \text{Dy}_2\text{Cu}_2\text{Cd} + (1-x) \text{Tm}_2\text{Cu}_2\text{Cd}$ composite materials, $\Delta S_{\text{comp}}(T, H, x)$, can be calculated theoretically from the individual $\Delta S_M(T)$ curves^{35–38},

$$\Delta S_{\text{comp}}(T, H, x) = x \Delta S_{\text{Dy}}(T, H) + (1-x) \Delta S_{\text{Tm}}(T, H), \quad (2)$$

where x and $1-x$ are the weight amounts of $\text{Dy}_2\text{Cu}_2\text{Cd}$ and $\text{Tm}_2\text{Cu}_2\text{Cd}$, respectively. Based on both compounds, a composite material can be formed and the optimum ratio of $x \sim 0.77$ is determined by using a numerical method. The magnetic entropy change $\Delta S_{\text{comp}}(T)$ for $\text{Dy}_2\text{Cu}_2\text{Cd} - \text{Tm}_2\text{Cu}_2\text{Cd}$ composite material at $x \sim 0.77$ under a magnetic field change of 0–50 kOe is shown in Fig. 9. A table-like MCE in a wide temperature span of

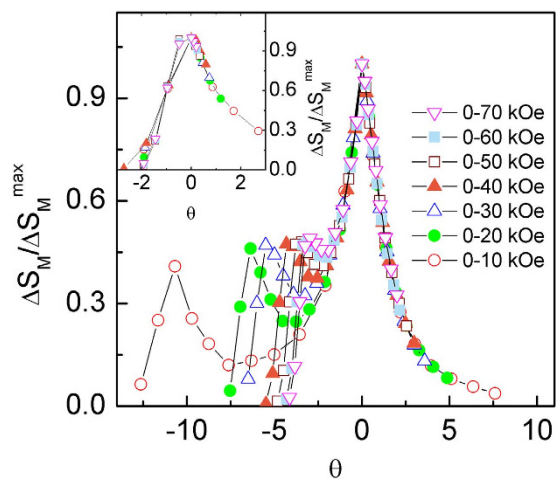


Figure 7. Normalized magnetic entropy change $\Delta S'_M (= \Delta S_M / \Delta S_M^{\max})$ as a function of the rescaled temperature θ around T_C for Dy_2Cu_2Cd compound. Inset shows the normalized magnetic entropy change $\Delta S'_M (= \Delta S_M / \Delta S_M^{\max})$ as a function of the rescaled temperature θ around T_S for Dy_2Cu_2Cd compound.

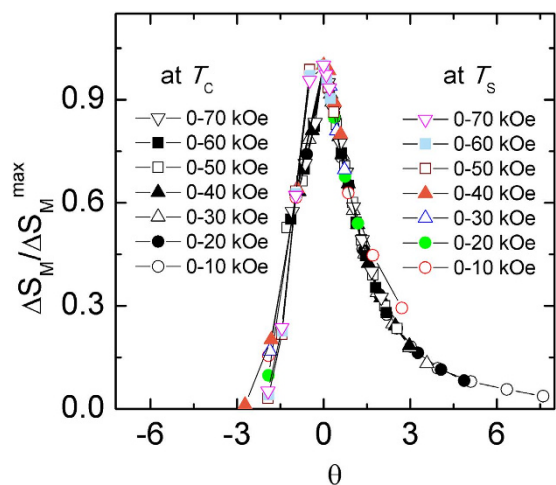


Figure 8. Normalized magnetic entropy change $\Delta S'_M (= \Delta S_M / \Delta S_M^{\max})$ as a function of the rescaled temperature θ around T_C and T_S for Dy_2Cu_2Cd compound.

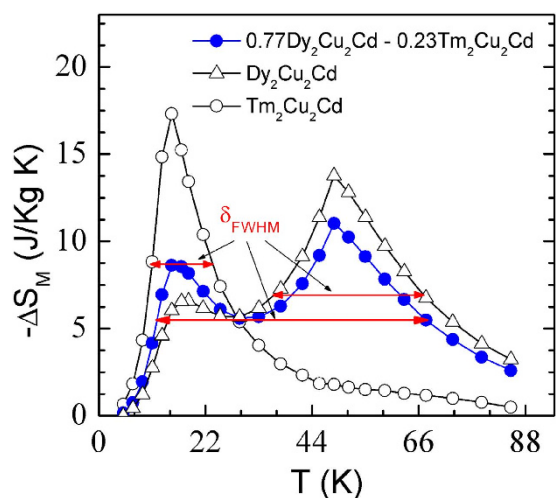


Figure 9. Temperature dependence of magnetic entropy change $-\Delta S_{\text{comp}}$ for the 0.77 Dy_2Cu_2Cd - 0.23 Tm_2Cu_2Cd composite material for the magnetic field change of 0–50 kOe.

Material	T_C (K)	$-\Delta S_M^{\max}$ (J/kg K)	RC (J/kg)	Ref.
Dy ₂ Cu ₂ Cd	48.5/16	13.8	316	present
Tm ₂ Cu ₂ Cd	15	17.3	165	present
0.77Dy ₂ Cu ₂ Cd-0.23Tm ₂ Cu ₂ Cd		11.0	417	present
DyNi ₂ B ₂ C	10	17.1	~182	39
ErAgAl	14	10.5	~196	40
Dy ₂ CoGa ₃	17	10.8	252	41
Ho ₂ Au ₂ In	21	12.9	~261	23
HoPdIn	23	14.6	~372	24
TbCo ₃ B ₂	28	8.7	~215	42
Ho ₂ Cu ₂ In	30	17.4	~320	23
EuAuGe	33	7.6	~269	43
Tm ₂ Cu ₂ In	39.4	14.4	260	21
EuAuZn	52	9.1	~239	44
Tb ₃ Ni ₆ Al ₂	57.5	9.8	~346	45
Dy ₁₂ Co ₇	64	10.0	299	46

Table 1. The transition temperature T_C , the maximum values of magnetic entropy change $-\Delta S_M^{\max}$ and refrigeration capacity RC under the magnetic field change of 0–50 kOe for Dy₂Cu₂Cd and Tm₂Cu₂Cd as well as the 0.77Dy₂Cu₂Cd - 0.23Tm₂Cu₂Cd composite material together with some MCE materials with the T_C from 10 to 70 K.

10–70 K can be observed in $\Delta S_{\text{comp}}(T)$ curve which is desirable for an ideal Ericsson-cycle magnetic refrigeration. The corresponding maximum value of RC_{comp} is 417 J/kg, which is 32% and 153% higher than those of Dy₂Cu₂Cd (316 J/kg) or Tm₂Cu₂Cd (165 J/kg). The transition temperature T_C , the maximum values of $-\Delta S_M^{\max}$ and RC under the magnetic field change of 0–50 kOe for Dy₂Cu₂Cd and Tm₂Cu₂Cd as well as the 0.77 Dy₂Cu₂Cd - 0.23 Tm₂Cu₂Cd composite material together with some MCE materials in the similar working temperature range are listed in Table 1 for comparison. The MCE parameters for the present studied materials are comparable or larger than those of other potential magnetic refrigerant materials in the similar temperature region, suggesting RE₂Cu₂Cd composite materials could be a promising candidate for magnetic refrigeration for Ericsson cycle in the temperature range of 10–70 K. The present results allow for the possibility of using RE₂Cu₂Cd compounds to fabricate composite materials with desirable magnetocaloric properties for active magnetic refrigeration.

Conclusions

In summary, two single phased Dy₂Cu₂Cd and Tm₂Cu₂Cd compounds have been fabricated and the magnetism and magnetocaloric effect have been investigated experimentally. Both compounds undergo a paramagnetic to ferromagnetic transition at their own Curie temperatures, additionally, another magnetic transition is also observed for Dy₂Cu₂Cd at low temperatures. For a magnetic field change of 0–50 kOe, the maximum values of magnetic entropy change ($-\Delta S_M^{\max}$) are 13.8 J/kg K around T_C , and 6.6 J/kg K around T_S for Dy₂Cu₂Cd; and 17.3 J/kg K for Tm₂Cu₂Cd, respectively. The rescaled entropy change ΔS_M curves around T_C follow a universal behaviour for Dy₂Cu₂Cd and Tm₂Cu₂Cd, which further confirm both compounds with the second order phase transition. A table-like MCE from 10 to 70 K and a strong enhancement of RC have been found in theoretically calculated Dy₂Cu₂Cd-Tm₂Cu₂Cd composite materials. The maximum value of RC_{comp} is 417 J/kg in the 0.77Er₂Cu₂Cd - 0.23Tm₂Cu₂Cd composite material for a magnetic field change of 0–50 kOe, which is obviously larger than those for either Dy₂Cu₂Cd (316 J/kg) or Tm₂Cu₂Cd (165 J/kg) compounds. The results indicate that the RE₂Cu₂Cd (RE = Dy and Tm) compounds and its composite materials could be promising candidates for magnetic refrigeration in the temperature range of 10–70 K. Furthermore, the present results may also provide a cost-effective strategy for exploring suitable refrigeration candidates with table-like magnetocaloric feature by a materials composition method, beneficial for Ericsson-cycle in the wide temperature range.

Methods

The Dy₂Cu₂Cd and Tm₂Cu₂Cd polycrystalline samples were fabricated by induction melting the elements in a sealed quartz crucible. Firstly, high purity Dy, Tm, Cu and Cd with stoichiometric amounts were weighted and placed in the quartz crucible. Secondly, a high vacuum better than 2×10^{-5} mbar was achieved in the crucible. Then the crucible was filled with purified argon gas at pressure of ca. 750 mbar and sealed immediately. Finally, the quartz crucible was placed in an induction furnace and heated at 1100 K for 4 minutes, following by 3 hours annealing at 850 K. The powder X-ray diffraction (Bruker D8 Advance) measurements were carried out at room temperature using Cu $K\alpha$ radiation. Both samples were proved to be single phase, and the lattice parameters were evaluated to be $a = 7.491$ and $c = 3.742$ Å for Dy₂Cu₂Cd; and to be $a = 7.439$ and $c = 3.687$ Å for Tm₂Cu₂Cd, respectively. The magnetic measurements were performed by using a commercial vibrating sample magnetometer (VSM) which is an option of the physical properties measurement system (PPMS-9, Quantum Design) in the temperature range of 3–298 K with a DC magnetic field from 0 to 7 T, and the samples are small particles of 4.5 and 3.8 mg for Dy₂Cu₂Cd and Tm₂Cu₂Cd, respectively.

References

- Gschneidner, A., Pecharsky, V. K. & Tsokol, A. O. Recent developments in magnetocaloric materials. *Rep. Prog. Phys.* **68**, 1479 (2005).
- Tishin, A. M. Magnetocaloric effect: Current situation and future trends. *J. Magn. Magn. Mater.* **316**, 351 (2007).
- Li, L. W. Review of magnetic properties and magnetocaloric effect in the intermetallic compounds of rare earth with low boiling point metals. *Chin. Phys. B* **25**, 037502 (2016).
- Shen, B. G., Sun, J. R., Hu, F. X., Zhang, H. W. & Cheng, Z. H. Recent progress in exploring magnetocaloric materials. *Adv. Mater.* **21**, 4545 (2009).
- Franco, V., Blazquez, J. S., Ingale, B. & Conde, A. The magnetocaloric effect and magnetic refrigeration near room temperature: materials and models. *Annu. Rev. Mater. Res.* **42**, 305 (2012).
- Palacios, E. *et al.* Effect of Gd polarization on the large magnetocaloric effect of GdCrO₄ in a broad temperature range. *Phys. Rev. B* **93**, 064420 (2016).
- Liu, E. K. *et al.* Stable magnetostructural coupling with tunable magnetoresponse effects in hexagonal ferromagnets. *Nat. Commun.* **3**, 873 (2012).
- Liu, J., Gottschall, T., Skokov, K. P., Moore, J. D. & Gutfleisch, O. Giant magnetocaloric effect driven by structural transitions. *Nat. Mater.* **11**, 620 (2012).
- Tegus, O., Brück, E., Buschow, K. H. J. & Boer, de F. R. Transition-metal-based magnetic refrigerants for room-temperature applications. *Nature (London)* **415**, 150 (2002).
- Hu, F. X. *et al.* Influence of negative lattice expansion and metamagnetic transition on magnetic entropy change in the compound LaFe_{11.4}Si_{1.6}. *Appl. Phys. Lett.* **78**, 3675 (2001).
- Li, L. *et al.* Giant low field magnetocaloric effect and field-induced metamagnetic transition in TmZn. *Appl. Phys. Lett.* **107**, 132401 (2015).
- Zhang, Y. K., Wilde, G., Li, X., Ren, Z. & Li, L. Magnetism and magnetocaloric effect in the ternary equiatomic REFeAl (RE = Er and Ho) compounds. *Intermetallics* **65**, 61 (2015).
- Li, L. W. *et al.* Giant reversible magnetocaloric effect in ErMn₂Si₂ compound with a second order magnetic phase transition. *Appl. Phys. Lett.* **100**, 152403 (2012).
- Ke, Y. J., Zhang, X. Q., Ma, Y. & Cheng, Z. H. Anisotropic magnetic entropy change in RFeO₃ single crystals (R = Tb, Tm, or Y). *Sci. Rep.* **6**, 19775 (2016).
- Monteiro, J. C. B., Reis, R. D. dos & Gandra, F. G. The physical properties of Gd₃Ru: A real candidate for a practical cryogenic refrigerator. *Appl. Phys. Lett.* **106**, 194106 (2015).
- Li, L. & Nishimura, K. Giant reversible magnetocaloric effect in antiferromagnetic superconductor Dy_{0.9}Tm_{0.1}Ni₂B₂C compound. *Appl. Phys. Lett.* **95**, 132505 (2009).
- Jang, D. *et al.* Large magnetocaloric effect and adiabatic demagnetization refrigeration with YbPt₂Sn. *Sci. Rep.* **6**, 8680 (2015).
- Rieger, W., Nowotny, H. & Benesovsky, F. Die kristallstruktur von Mo₃FeB₂. *Monatsh. Chem.* **95**, 1502 (1964).
- Tappe, F. & Pöttgen, R. Rare earth-transition metal-cadmium intermetallics - crystal chemistry and physical properties. *Rev. Inorg. Chem.* **31**, 5 (2011).
- Schappacher, F. M., Hermes, W. & Pöttgen, R. Structure and magnetic properties of RE₂Cu₂Cd. *J. Solid State Chem.* **182**, 265 (2009).
- Zhang, Y. K. *et al.* Large reversible magnetocaloric effect in RE₂Cu₂In (RE = Er and Tm) and enhanced refrigerant capacity in its composite materials. *J. Phys. D: Appl. Phys.* **49**, 145002 (2016).
- Zhang, Y. *et al.* Study of the magnetic phase transitions and magnetocaloric effect in Dy₂Cu₂In compound. *J. Alloys Compd.* **667**, 130 (2016).
- Li, L. *et al.* Magnetic properties and large magnetocaloric effect in Ho₂Cu₂In and Ho₂Au₂In compounds. *J. Mater. Sci.* **51**, 5421 (2016).
- Li, L. W., Namiki, T., Huo, D., Qian, Z. & Nishimura, K. Two successive magnetic transitions induced large refrigerant capacity in HoPdIn compound. *Appl. Phys. Lett.* **103**, 222405 (2013).
- Zhang, Q., Cho, J. H., Li, B., Hu, W. J. & Zhang, Z. D. Magnetocaloric effect in Ho₂In over a wide temperature range. *Appl. Phys. Lett.* **94**, 182501 (2009).
- Banerjee, B. K. On a generalised approach to first and second order magnetic transitions. *Phys. Lett.* **12**, 16 (1964).
- Bingham, N. S., Phan, M. H., Srikanth, H., Torija, M. A. & Leighton, C. Magnetocaloric effect and refrigerant capacity in charge-ordered manganites. *J. Appl. Phys.* **106**, 023909 (2009).
- Franco, V., Blazquez, J. S. & Conde, A. Field dependence of the magnetocaloric effect in materials with a second order phase transition: A master curve for the magnetic entropy change. *Appl. Phys. Lett.* **89**, 222512 (2006).
- Franco, V., Conde, A., Romero-Enrique, J. M. & Blazquez, J. S. A universal curve for the magnetocaloric effect: an analysis based on scaling relations. *J. Phys.: Condens. Matter* **20**, 285207 (2008).
- Li, L. W., Yuan, Y., Zhang, Y., Pöttgen, R. & Zhou, S. Magnetic phase transitions and large magnetic entropy change with a wide temperature span in HoZn. *J. Alloys Compd.* **643**, 147 (2015).
- Li, Y. *et al.* Successive magnetic transitions and magnetocaloric effect in Dy₃Al₂ compound. *J. Alloys Compd.* **651**, 278 (2015).
- Zimm, C. *et al.* Description and performance of a near-room temperature magnetic refrigerator. *Adv. Cryogen. Eng.* **43**, 1759 (1998).
- Smaïli, A. & Chahine, R. Composite materials for Ericsson-like magnetic refrigeration cycle. *J. Appl. Phys.* **81**, 824 (1997).
- Li, L., Niehaus, O., Kersting, M. & Pöttgen, R. Reversible table-like magnetocaloric effect in Eu₁PdMg over a very large temperature span. *Appl. Phys. Lett.* **104**, 092416 (2014).
- Caballero-Flores, R., Franco, V., Aonde, A., Knippling, K. E. & Willard, M. A. Optimization of the refrigerant capacity in multiphase magnetocaloric materials. *Appl. Phys. Lett.* **98**, 102505 (2011).
- Chaturvedi, A., Stefanoski, S., Phan, M. H., Nolas, G. S. & Srikanth, H. Table-like magnetocaloric effect and enhanced refrigerant capacity in Eu₈Ga₁₆Ge₃₀-EuO composite materials. *Appl. Phys. Lett.* **99**, 162513 (2011).
- Alvarez, P., Llamazares, J. L. S., Gorria, P. & Blanco, J. A. Enhanced refrigerant capacity and magnetic entropy flattening using a two-amorphous FeZrB (Cu) composite. *Appl. Phys. Lett.* **99**, 232501 (2011).
- Li, L. W. *et al.* Low field giant magnetocaloric effect in RNiBC (R = Er and Gd) and enhanced refrigerant capacity in its composite materials. *Appl. Phys. Lett.* **101**, 122401 (2012).
- Li, L. *et al.* Large magnetic entropy change in Dy_{1-x}Ho_xNi₂B₂C (x = 0–1) superconductors. *Appl. Phys. Express* **4**, 093101 (2011).
- Zhang, Y., Yang, B. & Wilde, G. Magnetic properties and magnetocaloric effect in ternary REAgAl (RE = Er and Ho) intermetallic compounds. *J. Alloys Compd.* **619**, 12 (2015).
- Wang, L. C. *et al.* Large magnetocaloric effect with a wide working temperature span in the R₂CoGa₃ (R = Gd, Dy, and Ho) compounds. *J. Appl. Phys.* **115**, 233913 (2014).
- Li, L. W., Nishimura, K., Huo, D., Qian, Z. H. & Namiki, T. Critical behavior of the RCo₃B₂ (R = Gd, Tb and Dy) compounds. *J. Alloys Compd.* **572**, 205 (2013).
- Zhang, Y. & Wilde, G. Large reversible table-like magnetocaloric effect in EuAuGe compound. *J. Supercond. Nov. Magn.* **8**, 2159–2163 (2016).
- Li, L., Niehaus, O., Gerke, B. & Pöttgen, R. Magnetism and Magnetocaloric effect in EuAuZn. *IEEE Trans. Magn.* **50**, 2503604 (2014).
- Li, D. X., Nimori, S. & Aoki, D. Magnetic entropy change and relative cooling power of Gd₃Ni₆Al₂ and Tb₃Ni₆Al₂ compounds. *Solid State Commun.* **156**, 54 (2013).
- Dong, Q. Y. *et al.* Magnetic phase transition and magnetocaloric effect in Dy₁₂Co₇ compound. *J. Appl. Phys.* **114**, 173911 (2013).

Acknowledgements

The present work was partially supported by the National Natural Science Foundation of China (No. 51501036). Y. K. Zhang acknowledges the Alexander von Humboldt (AvH) Foundation for support with a post-doctoral fellowship.

Author Contributions

Y.Z. designed the study. Y.Y., X.X., S.G. and L.H. prepared the samples and performed the magnetocaloric measurements. Z.R., X.L. and G.W. provided suggestions for the data analyses and the manuscript. Y.Z. prepared the manuscript and all authors reviewed the manuscript.

Additional Information

Competing financial interests: The authors declare no competing financial interests.

How to cite this article: Zhang, Y. *et al.* Excellent magnetocaloric properties in RE_2Cu_2Cd ($RE = Dy$ and Tm) compounds and its composite materials. *Sci. Rep.* **6**, 34192; doi: 10.1038/srep34192 (2016).



This work is licensed under a Creative Commons Attribution 4.0 International License. The images or other third party material in this article are included in the article's Creative Commons license, unless indicated otherwise in the credit line; if the material is not included under the Creative Commons license, users will need to obtain permission from the license holder to reproduce the material. To view a copy of this license, visit <http://creativecommons.org/licenses/by/4.0/>

© The Author(s) 2016